Subramanyan Vasudevan
Jothinathan Lakshmi
Ganapathy Sozhan

Central Electrochemical Research Institute (CSIR), Karaikudi 630 006, Tamilnadu, India

Research Article

Studies on the Removal of Arsenate by Electrochemical Coagulation Using Aluminum Alloy Anode

The removal of arsenate from aqueous solution was carried out by electrochemical coagulation using aluminum alloy as anode and stainless steel as cathode. Various operating parameters on the removal efficiency of arsenate were investigated, such as initial arsenate ion concentration, initial pH, current density, and temperature. Effect of coexisting anions such as silicate, fluoride, phosphate, and carbonate were studied on the removal efficiency of arsenate. The optimum removal efficiency of 98.4% was achieved at a current density of 0.2 A/dm^2 at a pH of 7.0. The experimental data were tested against different adsorption isotherm models for describing the electrochemical coagulation process. The adsorption of arsenate preferably fitting the Langmuir adsorption isotherm suggests monolayer coverage of adsorbed molecules. First and second order rate equations were applied to study adsorption kinetics. The adsorption process follows second order kinetics model with good correlation. Temperature studies showed that adsorption was endothermic and spontaneous in nature.

Keywords: Adsorption kinetics; Arsenate removal; Electrochemical coagulation; Isotherms

Received: January 18, 2010; *revised:* April 19, 2010; *accepted:* April 22, 2010

DOI: 10.1002/clen.201000001

1 Introduction

Many pollutants in water streams have been identified as toxic and harmful to environment and human health. Among them, arsenic is considered as a high priority one. It occurs naturally in rocks and soils, water, air, plants, and animals. Volcanic activity, the erosion of rocks and minerals, and forest fires are also sources that can release arsenic into the environment [1, 2]. The other sources of arsenic are metallurgical industries, glassware and ceramic production, tannery operation, dyestuff, pesticide industries, some organic and inorganic chemical manufacturing, petroleum refining, and rare earth metals [3]. In natural waters, arsenic exists predominantly in inorganic form, as trivalent arsenite, As(III), and pentavalent arsenate As(V), while organic forms of arsenic are rarely quantitatively important [2]. The stability and dominance of arsenic compounds depend directly on the pH of solution. Pentavalent arsenic is stable at pH 0–2 as neutral H_3AsO_4, while $H_2AsO_4^-$, $HAsO_4^{2-}$, and AsO_4^{3-} exist as stable species in the pH interval 3–6, 7–11, and 12–14, respectively [4]. Pollution-based studies have shown that arsenate may adversely affect several organs in the human body including cancer of the skin, lung, and urinary bladder. Environmental protection agency lowered the maximum concentration level of arsenic in water system to 10 ppb [5]. Consequently, the removal of arsenic from water system becomes vital in order to comply with the legislation [6]. Various treatment methods have been developed for the removal of arsenic from water streams, such as sorption and ion exchange, precipitation, coagulation and flocculation, reverse osmosis, membrane technologies, electrodialysis, biological processes, as well as lime softening, etc. Among them, coagulation-precipitation followed by filtration has been recognized as a popular one. Reverse osmosis and electrodialysis have also been found effective, but they were costly and water recovery was not optimized. Co-precipitation/adsorption processes are commonly applied today to meet the current drinking water standards and show a good efficiency to cost ratio for higher arsenic concentrations. However, they fail to remove arsenic to concentrations below the new decreased limits (10 μg/L) [7–14]. During the last few decades, electrochemical water treatment technologies have undergone rapid growth and development. One of these technologies is the electrochemically-assisted coagulation that can compete with the conventional chemical coagulation process. The electrochemical production of destabilization agents that bring about charge neutralization from pollutant removal and it has been used for water or wastewater treatment. Usually iron and aluminum plates are used as electrodes in the electrocoagulation followed by electrosorption process [15–18]. Electrochemically generated metallic ions from these electrodes undergo hydrolysis near the anode to produce a series of activated intermediates that are able to destabilize the finely dispersed particles present in the water and waste water to be treated. The advantages of electrocoagulation include high particulate removal efficiency, a compact treatment facility, relatively low cost, and the possibility of complete

Correspondence: Dr. S. Vasudevan, Central Electrochemical Research Institute (CSIR), Karaikudi 630 006, Tamilnadu, India.
E-mail: vasudevan65@gmail.com

Abbreviation: **SEM**, scanning electron microscope.

automation [19–24]. This technique does not require supplementary addition of chemicals and reduces the volume of produced sludge.

(i) When Aluminum is used as electrode, the reactions are as follows:

$$\text{At the cathode}: \ 2\,H_2O + 2\,e^- \rightarrow H_2(g) + 2\,OH^- \quad (1)$$

$$\text{At the anode}: \ Al \rightarrow Al^{3+} + 3\,e^- \quad (2)$$

$$\text{In the solution}: \ Al^{3+}(aq) + 3\,H_2O \rightarrow Al(OH)_3 + 3\,H^+(aq) \quad (3)$$

(ii) When iron is used as electrode, the reactions are as follows:

$$\text{At the cathode}: \ 2\,H_2O + 2\,e^- \rightarrow H_2(g) + 2\,OH^- \quad (4)$$

$$\text{At the anode}: 4\,Fe(s) \rightarrow 4\,Fe^{2+}(aq) + 8\,e^- \quad (5)$$

$$\text{In the solution}: 4\,Fe(s) + 10\,H_2O(l) + O_2(g) \rightarrow Fe(OH)_3(s) + 4\,H_2(g) \quad (6)$$

This method is characterized by reduced sludge production, a minimum requirement of chemicals, and ease of operation. Although, there are numerous reports related to electrochemical coagulation as a means of removal of arsenate using iron as anode material from water and wastewater [20–22], but there are limited work on arsenate removal by electrochemical coagulation using aluminum alloy as anode and its adsorption and kinetics studies [23]. This article presents the results of the laboratory scale studies on the removal of arsenate using aluminum alloy and stainless steel as anode and cathode, respectively, by electrochemical coagulation process. In doing so, the equilibrium adsorption behavior is analyzed by fitting models of Langmuir, Freundlich, Dubinin–Redushkevich, and Frumkin isotherms. Adsorption kinetics of electrocoagulants is analyzed using first- and second order kinetic models. Activation energy is evaluated to study the nature of adsorption. In natural water, some places, arsenic exists with other ions such as carbonate, silicate, phosphate, and fluoride. Hence, the effect of coexisting ions was also studied on the removal efficiency of arsenate.

2 Experimental

2.1 Cell Construction and Electrolysis

A laboratory scale batch electrolytic cell (Fig. 1) made of Plexiglas was used in all electrocoagulation experiments. Aluminum alloy (consisting of Zn (1–4%), In (0.006–0.025%), Fe (0.15%), Si (0.15%) [CECRI, (CSIR), India], with a surface area of 0.2 dm^2 acted as the anode. The cathodes were a stainless steel (SS 304; SAIL, India; consisting of <0.08% C, 17.5–20% Cr, 8–11% Ni, <2% Mn, <1% Si, <0.045% P, <0.03% S) sheets of the same size as the anode is placed at an interelectrode distance of 0.005 m. The temperature of the electrolyte has been controlled to the desired value with a variation of ±2 K by adjusting the rate of flow of thermostatically controlled water through an external glass-cooling spiral. A regulated direct current (DC) was supplied from a rectifier (10 A, 0–25 V; Aplab model).

The arsenate ($Na_2HAsO_4{\cdot}7\,H_2O$) (Analar Reagent) was dissolved in distilled water for the required concentration (0.5–1.5 mg/L). The solution of 0.90 L was used for each experiment, which was used as the electrolyte. The pH of the electrolyte was adjusted, if required, with 1 M HCl or 1 M NaOH solutions before adsorption experiments. To study the effect of coexisting ions, in the removal of As(V), sodium

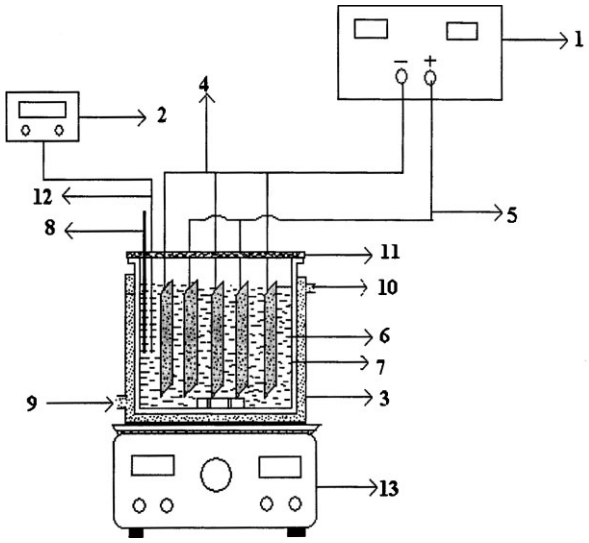

Figure 1. 1, DC power supply; 2, pH meter; 3, electrochemical cell; 4, cathodes; 5, anode; 6, electrolyte; 7, outer jacket; 8, thermostat; 9, inlet for thermostatic water; 10, outlet for thermostatic water; 11, PVC cover; 12, pH sensor; and 13, magnetic stirrer.

salts (Analar Grade) of phosphate (5–50 mg/L), silicate (5–15 mg/L), carbonate (5–250 mg/L), and fluoride (0.2–5 mg/L) was added to the electrolyte.

2.2 Analysis

Ion Chromatography (Metrohm AG, Switzerland) was used to determine the concentration of arsenate. The scanning electron microscope (SEM) and EDAX of aluminum hydroxide were analyzed with a SEM made by Hitachi (model s-3000h). The Fourier transform infrared spectrum of aluminum hydroxide was obtained using Nexus 670 FTIR spectrometer made by Thermo Electron Corporation, USA. The XRD of electrocoagulatioan by-products were analyzed by a JEOL X-ray diffractometer (Type – JEOL, Japan). The XPS of electrocoagulation by-products were analyzed by a Multilab 2000 (Type – Thermoscientific, UK).

3 Results and Discussion

3.1 Effect of Current Density

The current density determines the electrocoagulant dosage rate at electrocoagulation processes. Thus, current density should have a significant impact on arsenate removal efficiency. To investigate the effect of current density, a series of experiment were carried out using 0.5 mg/L of arsenate containing electrolyte, at a pH 7.0, with the current density being varied from 0.05 to 0.4 A/dm^2. The removal efficiencies of arsenate are 94.0, 96.2, 98.4, 99.2, and 99.4% for current densities 0.05, 0.1, 0.2, 0.3, and 0.4 A/dm^2, respectively. It is found that, beyond 0.2 A/dm^2 the removal efficiency remains almost constant for higher current densities. So, further studies were carried out at 0.2 A/dm^2. The results showed that as current density increases, removal of arsenate also increases. This can be attributed to the increase in the amount of aluminum hydroxide being generated in situ thereby resulting in rapid removal of arsenate. The amount of adsorbent [$Al(OH)_3$] was determined from the

Faraday law [25]

$$E_c = I\ t\ M/Z\ F \quad (7)$$

where I is current in A, t the time (s), M the molecular weight, Z the electron involved, and F is the Faraday constant (96485.3 C/mol). As expected, the amount of arsenate adsorption increases with the increase in adsorbent concentration, which indicates that the adsorption depends up on the availability of binding sites for arsenate.

3.2 Effect of pH

It has been established that the solution pH has a considerable influence on the performance of electrochemical coagulation process. To evaluate this effect, a series of experiments were carried out using 0.5 mg/L arsenate containing solutions, with an initial pH varying in the range 1–11. The removal efficiency of arsenate was increased with increasing the pH up to 7. When the pH is above 7, removal efficiency should be slightly decreases. It is found that (Fig. 2) the maximum removal efficiency for the removal of arsenate is 98.4% at pH 7 and the minimum efficiency is 93% at pH 1. The decrease of removal efficiency at more acidic and alkaline pH was observed by many investigators [19] and was attributed to an amphoteric behavior of $Al(OH)_3$ which leads to soluble Al^{3+} cations (at acidic pH) and to monomeric anions $Al(OH)_4^-$ (at alkaline pH). It is well known that these soluble species are not useful for water treatment. When the initial pH was kept in neutral, all the aluminum produced at the anode formed polymeric species ($Al_{13}O_4(OH)_{24}^{7+}$) and precipitated $Al(OH)_3$ leading to more removal efficiency. In the present study, the results agree well with the results presented in the literature and the maximum amount of arsenate removal occurred at pH 7.0 [25].

3.3 Effect of Initial Arsenate Concentration

In order to evaluate the effect of initial arsenate concentration, experiments were conducted at varying initial concentration from 0.5 to 1.5 mg/L. Figure 3 shows that the uptake of arsenate (mg/g) increased with increase in arsenate concentration and remained nearly constant after equilibrium time. The equilibrium time was found to be 30 min for all concentrations studied. The amount of arsenate adsorbed (q_e) increased from 0.474 to 1.4 mg/g as the concentration increased from 0.5 to 1.5 mg/L. From the figure it is observed that the adsorption is the rapid in the initial stages and gradually decreases with progress of adsorption. The plots are single, smooth, and continuous curves leading to saturation, suggesting the possible monolayer coverage to arsenate on the surface of the adsorbent [26, 27].

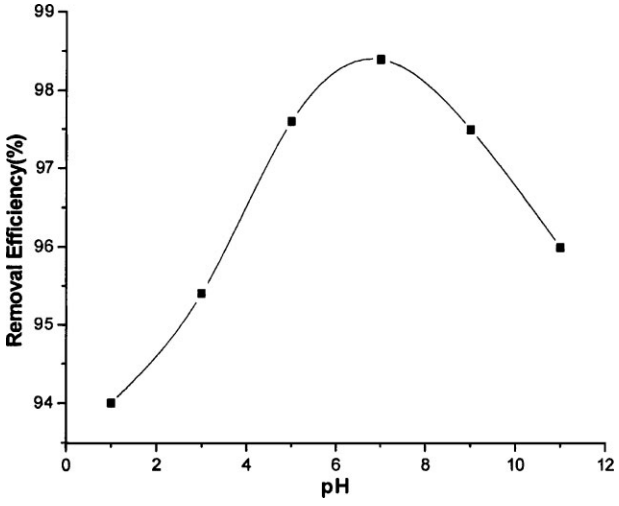

Figure 2. Effect of pH of the electrolyte on the removal of arsenate. Conditions: electrolyte concentration, 0.5 mg/L; current density, 0.2 A/dm^2; temperature, 303 K.

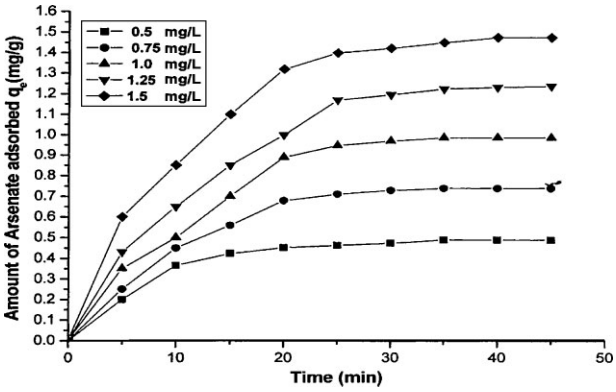

Figure 3. Effect of agitation time and amount of arsenate adsorbed. Conditions: current density, 0.2 A/dm^2; pH of the electrolyte, 7.0; temperature, 303 K.

3.4 Adsorption Kinetics

In order to establish kinetic of arsenate adsorption, adsorption kinetics of aluminum alloy was investigated by using first order, second order kinetic models, Elovich and intraparticle diffusion.

3.4.1 First Order Lagergren Model

The first order Lagergren model is generally expressed as follows [26, 28],

$$dq/dt = k_1(q_e - q_t) \quad (8)$$

where, q_t is the amount of arsenate adsorbed on the adsorbent at time t (min) and k_1 (1/min) is the rate constant of first order adsorption. The integrated form of the above equation with the boundary conditions $t = 0$ to $t = t$ and $q_t = 0$ to $q_t = q_t$ and then rearranged to obtain the following time dependence function:

$$\log(q_e - q_t) = \log(q_e) - k_1 t/2.303 \quad (9)$$

The values of log $(q_e - q_t)$ were linearly correlated with t, from which k_1 and q_e can be determined by the slope and intercept, respectively. A straight line obtained from the plots suggests the applicability of this kinetic model.

3.4.2 Second Order Lagergren Model

The second order kinetic model is expressed as [29]

$$dq/dt = k_2(q_e - q_t)^2 \quad (10)$$

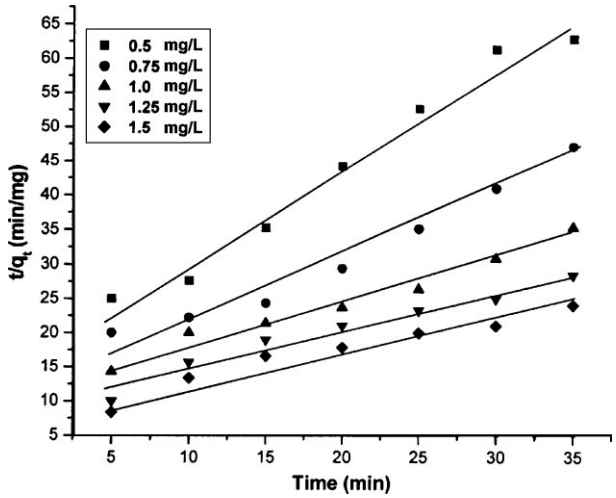

Figure 4. Second order kinetic model plot of different concentrations of arsenate. Conditions: current density, 0.2 A/dm^2; pH of the electrolyte, 7.0; temperature, 303 K.

Where k_2 is the rate constant of second order adsorption. The integrated form of Eq. (10) with the boundary condition $t = 0$ to >0 ($q = 0$ to >0) is

$$1/(q_e - q_t) = 1/q_e + k_2\, t \tag{11}$$

Eq. (11) can be rearranged and linearized as,

$$t/q_t = 1/k_2\, q_e^2 + t/q_e \tag{12}$$

The plot of t/q_t and time (t) (Fig. 4) should give a linear relationship from which q_e and k_2 can be determined from the slope and intercept of the plot, respectively. Table 1 depicts the computed results obtained from first order and second order.

3.4.3 Elovich Equation

The Elovich model equation is generally expressed as [30]

$$dq_t/dt = \alpha \exp(-\beta\, q_t) \tag{13}$$

the simplified form of Elovich Eq. (13) is

$$q_t = 1/\beta\ \log_e(\alpha\beta) + \Delta/\beta\ \log_e(\tau) \tag{14}$$

If arsenate adsorption fits the Elovich model, a plot of q_t versus $\log_e(t)$ should yield a linear relationship with the slope of $(1/\beta)$ and an intercept of $1/\beta\ \log_e(\alpha\beta)$.

3.4.4 Intraparticle Diffusion

The intraparticle diffusion model is expressed as [31, 32]

$$R = k_{id}(t)^{\alpha\zeta} \tag{15}$$

A linearized form in the Eq. (15) is followed by

$$\log R = \log\ k_{id} + a \log(t) \tag{16}$$

in which a depicts the adsorption mechanism and k_{id} may be taken as the rate factor (percent of arsenate adsorbed per unit time). Lower and higher value of k_{id} illustrates an enhancement in the rate of adsorption and better adsorption with improved bonding between pollutant and the adsorbent particles, respectively. Table 2 depicts the computed results obtained from Elovich and intraparticle diffusion.

From Tabs. 1 and 2 it is found that the correlation coefficient decreases from second order, first order, intraparticle diffusion to Elovich model. This indicates that the adsorption follows the second order than other models. The calculated q_e values also well agree with the experimental q_e values for second order kinetics model.

3.5 Adsorption Isotherm

The adsorption capacity of the adsorbent has been tested using Freundlich, Langmuir, Dubinin–Redushkevich, and Frumkin isotherms. These models have been widely used to describe the behavior of adsorbent–adsorbate couples. To determine the isotherms, the initial pH was kept at 7 and the concentration of arsenate used was in the range of 0.5–1.5 mg/L.

3.5.1 Freundlich Isotherm

The general form of Freundlich adsorption isotherm is represented by [33]

$$q_e = K\, C^n \tag{17}$$

Eq. (17) can be linearized in logarithmic form and the Freundlich constants can be determined as follows:

$$\log q_e = \log k_f + n\ \log C_e \tag{18}$$

where, k_f is the Freundlich constant related to adsorption capacity, n the energy or intensity of adsorption; C_e the equilibrium concentration of arsenate (mg/L). The values of k_f and n can be obtained by plotting logarithms of adsorption capacity against equilibrium concentrations. To determine the isotherms, the arsenate concentration used was 0.5–1.5 mg/L and at an initial pH 7. The Freundlich constants k_f and n values are 0.9417 mg/g and 1.0155 L/mg, respectively.

Table 1. Comparison between the experimental and calculated q_e values for different initial arsenate concentrations in first and second order adsorption isotherm at temperature 305 K and pH 7.

Concentration (mg/L)	q_e (exp)	First order adsorption			Second order adsorption		
		q_e (Cal)	$K_1 \times 10^4$ (min/mg)	R^2	q_e (Cal)	$K_2 \times 10^4$ (min/mg)	R^2
0.50	0.474	0.328	0.167	0.9817	0.471	0.1613	0.9926
0.75	0.711	0.441	0.123	0.9628	0.694	0.0682	0.9978
1.00	0.948	0.671	0.091	0.9932	0.899	0.0450	0.9997
1.25	1.171	0.993	0.089	0.9836	1.071	0.0371	0.9997
1.50	1.40	1.222	0.063	0.9772	1.266	0.0292	0.9992

Table 2. Elovich model and intraparticle diffusion for different initial arsenate concentrations at temperature 305 K and pH 7.

Concentration (mg/L)	Elovich model			Intraparticle diffusion		
	A (mg/g h)	B (g/mg)	R^2	K_{id} (1/h)	A (%/h)	R^2
0.50	9.32	62.31	0.962	36.71	0.124	0.982
0.75	2.37	41.36	0.951	33.23	0.156	0.961
1.00	0.91	24.28	0.942	29.37	0.211	0.973
1.25	0.73	18.36	0.969	28.42	0.326	0.982
1.50	0.61	9.27	0.977	25.38	0.451	0.979

It has been reported that values of n lying between 0 and 10 indicate favorable adsorption. From the analysis of the results it is found that the Freundlich plots fit satisfactorily with the experimental data obtained in the present study. This is well agreed with the results presented in the literature [34].

3.5.2 Langmuir Isotherm

The linearized form of Langmuir adsorption isotherm model is [35, 36]

$$C_e/q_e = 1/q_o\, b + C_e/q_o \tag{19}$$

where C_e is the concentration of the arsenate solution (mg/L) at equilibrium, q_o the adsorption capacity (Langmuir constant) and b is the energy of adsorption. Figure 5 shows the Langmuir plot with experimental data. The value of the adsorption capacity q_o as found to be 55.959 mg/g, which is higher than that of other adsorbents studied.

The essential characteristics of the Langmuir isotherm can be expressed as the dimensionless constant R_L.

$$R_L = 1/(1 + b\, C_o) \tag{20}$$

where R_L is the equilibrium constant it indicates the type of adsorption, b, C_o the Langmuir constant. The R_L values between 0 and 1 indicate the favorable adsorption. The R_L values were found to be between 0 and 1 for all the concentrations of arsenate studied. The results are presented in Tab. 3.

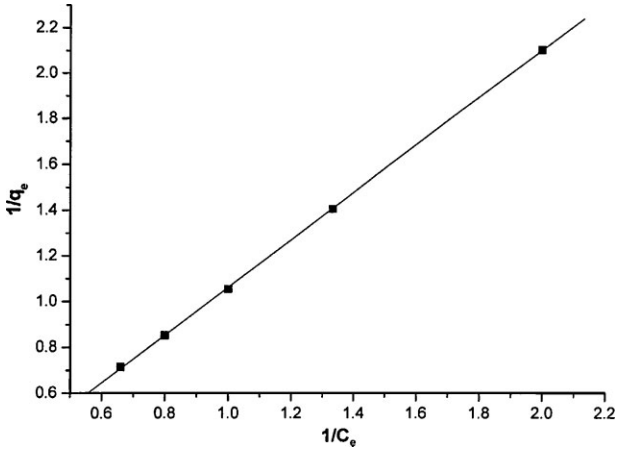

Figure 5. Langmuir plot ($1/q_e$ vs. $1/C_e$) for adsorption of arsenate. Conditions: pH of the electrolyte, 7.0; current density, 0.2 A/dm^2; temperature, 303 K; concentration, 0.5–1.5 mg/L.

3.5.3 Dubinin–Redushkevich (D–R) Isotherm

This isotherm model was chosen to estimate the characteristics porosity of the biomass and apparent energy of adsorption. This model is represented by the Eq. (21)

$$q_e = q_s \exp(-B\, \varepsilon^2) \tag{21}$$

where $\varepsilon = R\, T \ln[1 + 1/C_e]$, B is related to the free energy of sorption per mole of the adsorbate as it migrates to the surface of the biomass from infinite distance in the solution and q_s is the Dubinin–Redushkevich (D–R) isotherm constant related to the degree of adsorbate adsorption by the adsorbent surface [37]. The linearized form of the Eq. (21)

$$\ln q_e = \ln q_s - 2\, B\, R\, T\ \ln[1 + 1/C_e] \tag{22}$$

The isotherm constants of q_s and B are obtained from the intercept and slope of the plot of $\ln q_e$ versus ε^2, respectively [38]. The constant B gives the mean free energy (E), of adsorption per molecule of the adsorbate when it is transferred to the surface of the solid from infinity in the solution and the relation is given as

$$E = [1/\sqrt{2\, B}] \tag{23}$$

The magnitude of E is useful for estimating the type of adsorption process. It was found to be 18.28 kJ/mol, which is bigger than the energy range of adsorption reaction of 8–16 kJ/mol [39]. So the type of adsorption of As(V) on aluminum alloy was defined as chemical adsorption.

3.5.4 Frumkin Equation

Frumkin equation indicates the interaction between the adsorbed species. It can be expressed as

$$\theta/(1 - \theta)\ e^{-2a\theta} = \kappa\ C_e \tag{24}$$

where $\theta = q_e/q_m$, q_e is the adsorption capacity in equilibrium (mg/g) and q_m is the theoretical monolayer saturation capacity (mg/g). The linearized form is given as

$$\ln[(\theta/(1 - \theta))\ 1/C_e] = \ln k + 2\ a\theta \tag{25}$$

The parameters a and k are obtained from the slope and intercept of the plot $\ln[(\theta/(1-\theta))\ 1/C_e]$ versus θ. The constant k is related to adsorption equilibrium. The Frumkin equation has been specifically developed to take lateral interaction. The term $e^{-2a\theta}$ in Eq. (24) reflects the extent of lateral interaction, if $a > 0$ indicates attraction, while $a < 0$ means repulsion [40]. From Tab. 3, we see that the value $a > 0$ indicating attraction.

The correlation coefficient values of different isotherm models are listed in Tab. 3. The Langmuir isotherm model has higher regression

Table 3. Constant parameters and correlation coefficient calculated for different adsorption isotherm models at room temperature for arsenate adsorption at 0.5 mg/L.

	Isotherm		Constants	
	Q_o (mg/g)	b (L/mg)	R_L	R^2
Langmuir	55.959	0.0171	0.9831	0.9995
	Isotherm			Constants
	K_f (mg/g)	n (L/mg)		R^2
Freundlich	0.9417	1.0155		0.9894
	Isotherm		Constants	
	Q_s ($\times 10^3$ mol/g)	B ($\times 10^3$ mol^2 K/J^2)	E (kJ/mol)	R^2
D–R	1.192	1.495	18.28	0.9630
	Isotherm		Constants	
	a	ln k	$-\Delta G$ (kJ/mol)	R^2
Frumkin	−0.622	1.3770	806.52	0.9739

coefficient ($R^2 = 0.999$) when compared to the other models. The value of R_L for the Langmuir isotherm was calculated between 0 and 1, indicating the favorable adsorption of arsenate.

3.6 Thermodynamics Studies

The amount of arsenate adsorbed on the adsorbent increases by increasing the temperature indicating the process to be endothermic. The diffusion coefficient (D) for intraparticle transport of arsenate species into the adsorbent particles has been calculated at different temperature by

$$t_{1/2} = 0.03\ r_o^2/D \tag{26}$$

where $t_{1/2}$ is the time of half adsorption (s), r_o the radius of the adsorbent particle (20×10^{-4} cm), D the diffusion coefficient in cm^2/s. For all chemisorption system the diffusivity coefficient should be 10^{-5}–10^{-13} cm^2/s [41]. In the present work, D is found to be in the range of 10^{-10} cm^2/s. The pore diffusion coefficient (D) values for various temperatures and different initial concentrations of arsenate are presented in Tab. 4, respectively.

Table 4. Pore diffusion coefficients for the adsorption of arsenate at various concentration and temperature.

Concentration (mg/L)	Pore diffusion constant $D \times 10^{-9}$ (cm^2/s)
0.50	1.012
0.75	0.996
1.00	0.826
1.25	0.799
1.50	0.701
Temperature (K)	Pore diffusion constant $D \times 10^{-9}$ (cm^2/s)
313	1.114
323	1.021
333	0.936
343	0.812

To find out the energy of activation for adsorption of arsenate, the second order rate constant is expressed in Arrhenius form [42].

$$\ln k_2 = \ln k_o - E/R\,T \tag{27}$$

where k_o is the constant of the equation (g min/mg), E the energy of activation (J/mol), R the gas constant (8.314 J/mol K) and T the temperature in K. Figure 6 shows that the rate constants vary with temperature according to Eq. (27). The activation energy (12.37 kJ/mol) is calculated from slope of the fitted equation. The free energy change is obtained using the following relationship:

$$\Delta G = -R\,T\ \ln K_c \tag{28}$$

where ΔG is the free energy (kJ/mol), K_c the equilibrium constant, R the gas constant and T the temperature in K. The K_c and ΔG values are presented in Tab. 5. From the table it is found that the negative value of ΔG indicates the spontaneous nature of adsorption.

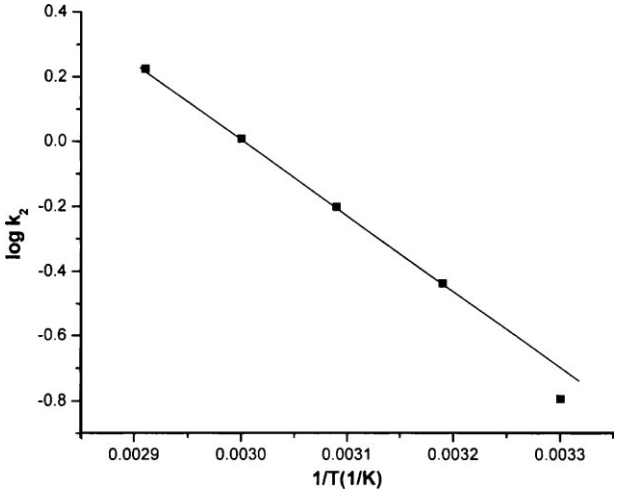

Figure 6. Plot of log k_2 and $1/T$ at pH of 7.0. Current density, 0.2 A/dm^2; temperature, 303 K; concentration, 0.5–1.5 mg/L.

Table 5. Thermodynamic parameters for the adsorption of arsenate.

Temperature (K)	K_c	ΔG^0 (J/mol)	ΔH^0 (kJ/mol)	ΔS^0 (J/mol K)
303	0.0096	−23.924		
313	0.0493	−127.64		
323	0.1294	−358.6	16.732	49.361
333	0.4561	−1341.7		
343	0.6671	−1955.16		

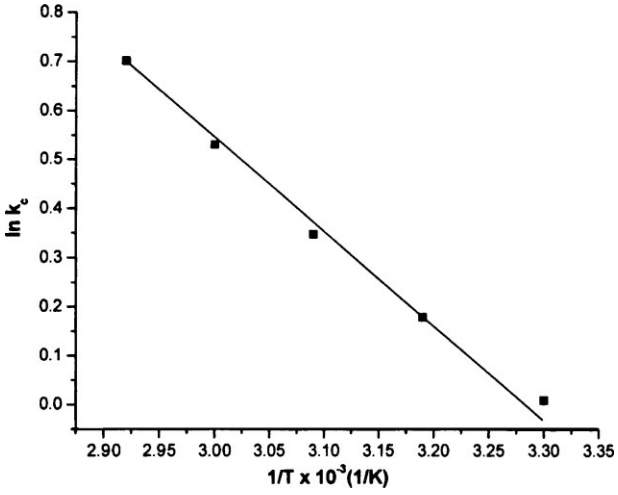

Figure 7. Plot of ln k_c and $1/T$. Conditions: pH of the electrolyte, 7.0; current density, 0.2 A/dm^2; temperature, 303 K; concentration, 0.5–1.5 mg/L.

Other thermodynamic parameters such as entropy change (ΔS) and enthalpy change (ΔH) were determined using van't Hoff equation

$$\ln K_c = \frac{\Delta \Sigma}{R} - \frac{\Delta H}{R\,T} \tag{29}$$

The enthalpy change ($\Delta H = 16.732$ kJ/mol) and entropy change ($\Delta S = 49.361$ J/mol K) were obtained from the slope and intercept of the van't Hoff linear plots of lnk_c versus $1/T$ (Fig. 7). A positive value of enthalpy change (ΔH) indicates that the adsorption process is endothermic in nature, and the negative value of change in internal energy (ΔG) shows the spontaneous adsorption of arsenate on the adsorbent. Positive values of entropy change show the increased randomness of the solution interface during the adsorption of arsenate on the adsorbent (Tab. 5). Enhancement of adsorption capacity of electrocoagulant (aluminum hydroxide) at higher temperatures may be attributed to the enlargement of pore size and or activation of the adsorbent surface. Using Lagergren rate equation, first order rate constants, and correlation coefficient were calculated for different temperatures (305–343 K). The calculated "q_e" values obtained from the second order kinetics agrees with the experimental "q_e" values better than the first order kinetics model. Table 6 depicts the computed results obtained from first and second order kinetic models. These results indicate that the adsorption follows second order kinetic model at different temperatures used in this study.

3.7 Effect of Coexisting Anions

3.7.1 Carbonate

Effect of carbonate on arsenate removal was evaluated by increasing the carbonate concentration from 5 to 250 mg/L in the electrolyte. The removal efficiencies are 98.4, 97.6, 70, 65, 20, and 15% for the carbonate ion concentration of 0, 2, 5, 65, 150, and 250 mg/L, respectively. From the results it is found that the removal efficiency of the arsenate is not affected by the presence of carbonate below 5 mg/L. Significant reduction in removal efficiency was observed above 5 mg/L of carbonate concentration is due to the passivation of anode resulting, the hindering of the dissolution process of anode.

3.7.2 Phosphate

The concentration of phosphate ion was increased from 5 to 50 mg/L, the contaminant range of phosphate in the ground water. The removal efficiency for arsenate was 98.4, 97.8, 60, 55, and 45% for 0, 2, 5, 25, and 50 mg/L of phosphate ion, respectively. There is no change in removal efficiency of arsenate below 5 mg/L of phosphate in the water. At higher concentrations (at and above 5 mg/L) of phosphate, the removal efficiency decreases drastically. This is due to the preferential adsorption of phosphate over arsenate as the concentration of phosphate increase.

3.7.3 Silicate

Effect of silicate on the removal efficiency of arsenate was studied. From the results it is found that the significant change in arsenate removal efficiency was observed. The respective efficiencies for 0, 5, 10, and 15 mg/L of silicate are 98.4, 54, 48, and 27%. The removal of arsenate decreased with increasing silicate concentration from 0 to 50 mg/ L. Further, increase in silicate concentration decreases the arsenate removal efficiency. In addition to preferential adsorption, silicate may interact with aluminum hydroxide to form soluble and highly dispersed colloids that are not removed by normal filtration.

3.7.4 Fluoride

From the results it is found that the efficiency decreased from 98.4 to 20% by increasing the concentration of fluoride from 0 to 5mg/L. Like

Table 6. Comparison between the experimental and calculated q_e values for initial arsenate concentration 0.5 mg/L in first and second order adsorption kinetics at various temperatures.

Temperature (K)	q_e (exp)	First order adsorption			Second order adsorption		
		q_e (Cal)	$K_1 \times 10^4$ (min/mg)	R^2	q_e (Cal)	$K_2 \times 10^4$ (min/mg)	R^2
313	0.474	0.226	0.167	0.9762	0.1613	0.467	0.9984
323	0.386	0.206	0.155	0.9645	0.1136	0.369	0.9963
333	0.268	0.199	0.148	0.9668	0.0854	0.253	0.9926
343	0.115	0.168	0.148	0.9865	0.0665	0.106	0.9965

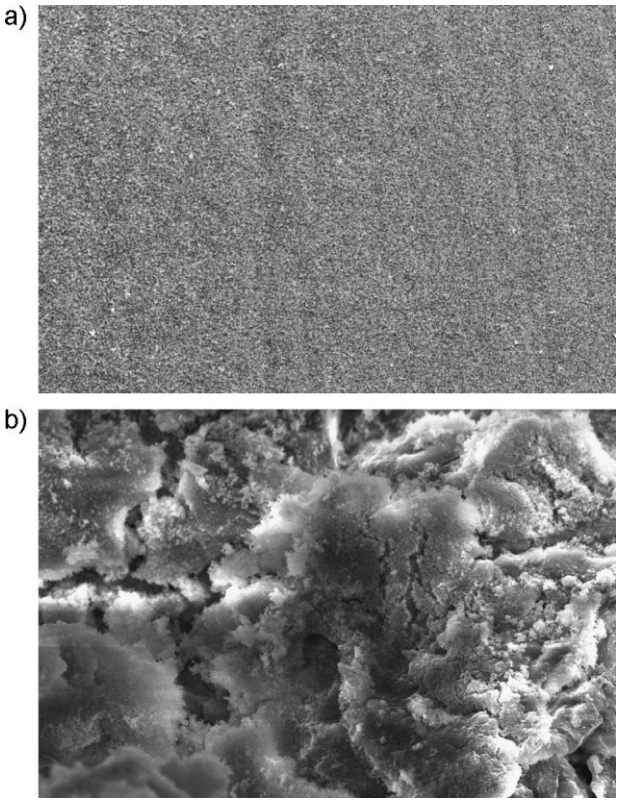

Figure 8. SEM image of the anode (a) before and (b) after treatment.

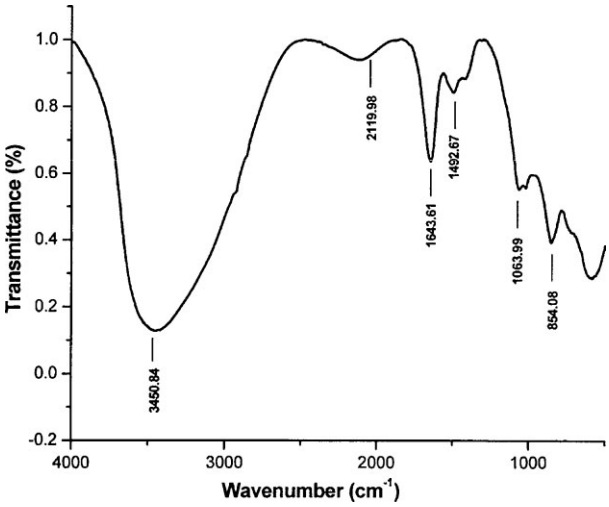

Figure 10. FTIR spectrum of arsenate-adsorbed aluminum hydroxide.

phosphate ion, this is due to the preferential adsorption of fluoride over arsenate as the concentration of fluoride increases. So, when fluoride ions are present in the water to be treated fluoride ions compete greatly with arsenate ions for the binding sites.

3.8 Material Characterization

3.8.1 SEM/EDAX Studies

SEM images of aluminum electrode, before and after, electrocoagulation of arsenate electrolyte was obtained to compare the surface texture. Figure 8a) shows the original aluminum plate surface prior to its use in electrocoagulation experiments. The surface of the electrode is uniform. Figure 8b) shows the SEM of the same electrode after several cycles of use in electrocoagulation experiments. The electrode surface is now found to be rough, with a number of dents. These dents are formed around the nucleus of the active sites where the electrode dissolution results in the production of aluminum hydroxides. The formation of a large number of dents may be attributed to the anode material consumption at active sites due to the generation of oxygen at its surface.

Energy-dispersive analysis of X-rays was used to analyze the elemental constituents of arsenate-adsorbed aluminum hydroxide shown in Fig. 9. It shows that the presence of arsenate appears in the spectrum other than the principal elements Al and O. EDAX analysis provides direct evidence that arsenate is adsorbed on aluminum hydroxide. Other elements detected in the adsorbed aluminum hydroxide come from adsorption of the conducting electrolyte, chemicals used in the experiments, alloying and the scrap impurities of the anode and cathode.

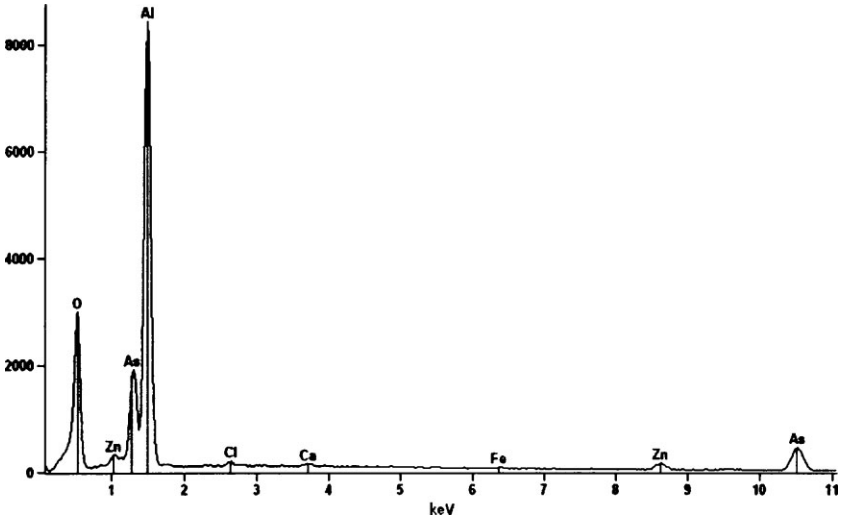

Figure 9. EDAX spectrum of arsenate-adsorbed aluminum hydroxide.

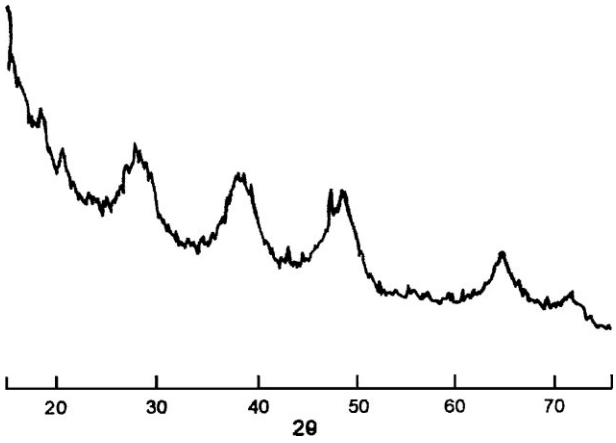

Figure 11. XRD spectrum of arsenate-adsorbed aluminum hydroxide.

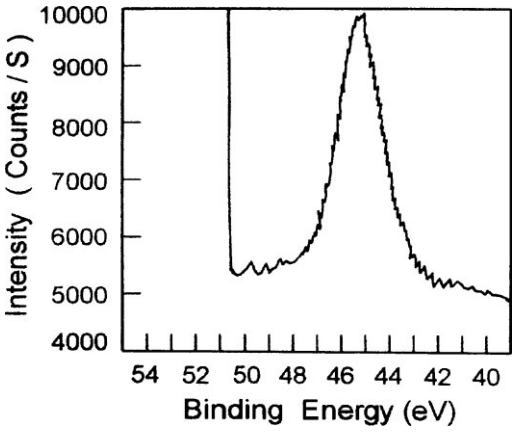

Figure 12. XPS spectrum of arsenate-adsorbed aluminum hydroxide.

3.8.2 FTIR Characterization

Figure 10 presents the FT-IR spectrum of arsenate–aluminum hydroxide. The sharp and strong peak at 3450.84 cm^{-1} is due to the O–H stretching vibration in the $Al(OH)_3$ structures. The 1643.61 cm^{-1} peak indicates the bent vibration of H–O–H. The strong peak at 926.00 cm^{-1} is assigned to the Al–O–H bending. As(V)–O vibration at 854 cm^{-1} also observed. The spectrum data are in good agreement with the reported data [43].

3.8.3 XRD Studies

X-ray diffraction spectrum of aluminum electrode coagulant showed very broad and sallow diffraction peaks (Fig. 11). This broad humps and low intensity indicate that the coagulant is amorphous or very poor crystalline in nature [43]. It is reported that the crystallization of aluminum hydroxide is a very slow process resulting all aluminum hydroxides found to be either amorphous or very poorly crystalline. The literature on the amorphous nature of aluminum oxide layer supported the present results.

3.8.4 XPS studies

The oxidation state of the arsenate in the coagulant was determined using XPS. It is reported that arsenate, As(V), has a 3D binding energy of 45.5 eV [44]. From the XPS spectra (Fig. 12) it is found that the As(V) treated coagulant exhibited a peak at 45.5 eV. The peak position was in close agreement with As(V) 3D binding energy reported in the literature [44].

4 Conclusions

The results showed that the optimized removal efficiency of 98.4% was achieved at a current density of 0.2 A/dm^2 and pH of 7.0 using aluminum alloy as anode and stainless steel as cathode. The aluminum hydroxide generated in the cell remove the arsenate present in the water and to reduce the arsenate concentration to 0.01 mg/L, and made it for drinking. The results indicate that the process can be scaled up to higher capacity. The adsorption of arsenate preferably fitting the Langmuir adsorption isotherm suggests monolayer coverage of adsorbed molecules. The adsorption process follows second order kinetics. Temperature studies showed that adsorption was endothermic and spontaneous in nature.

Acknowledgments

This work was financially supported by Chemical Engineering Programme of Department of Science and Technology, New Delhi, India. The authors wish to express their gratitude to the Director, Central Electrochemical Research Institute, Karaikudi to publish this paper.

References

[1] F. S. Zhang, H. Itoh, Iron Oxide Loaded Slag for Arsenic Removal From Aqueous Systems, *Chemosphere* **2005**, *60*, 319.

[2] M. Arienzo, P. Adamo, J. Chiarenzelli, M. R. Bianco, A. De Martino, Retention of Arsenic on Hydrous Ferric Oxides Generated by Electrochemical Peroxidation, *Chemosphere* **2002**, *48*, 1009.

[3] H. S. Altundogan, S. Altundogan, F. Tumen, M. Bildik, Arsenic Adsorption From Aqueous Solutions by Activated Red Mud, *Waste Manag.* **2002**, *22*, 357.

[4] T. Stanic, A. Dakavic, A. Zivanovic, M. Tomasevic-Canovic, V. Dondur, S. Milicevic, Adsorption of Arsenic(V) by Iron Modified Natural Zeolitic Tuff, *Environ. Chem. Lett.* **2008**, *7*, 14, 6975–7066.

[5] USEPA, National Primary Drinking Water Regulations; Arsenic and Clarification to Compliance and New Source Contaminants Monitoring Federal Register, Vol. 66, No. 14, Office of Water, USEPA, Washington **2001**, 6975–7066. www.rpa.gov

[6] B. Dousava, V. Machovic, D. Kolousek, F. Kovanda, V. Dornicak, Sorption of As(V) Species from Aqueous Systems, *Water Air Soil Pollut.* **2003**, *149*, 251.

[7] C. Namashivayam, S. Senthilkumar, Removal of Arsenic(V) from Aqueous Solution Using Industrial Solid Waste: Adsorption Rates and Equilibrium Studies, *Ind. Eng. Chem. Res.* **1998**, *37*, 4816.

[8] N. Seko, F. Basuki, M. Tamada, F. Yoshii, Rapid Removal of Arsenic(V) by Zirconium(IV) Loaded Phosphoric Chelate Adsorbent Synthesized by Radiation Induced Graft Polymerization, *React. Funct. Polym.* **2004**, *59*, 235.

[9] L. Zeng, A Method for Preparing Silica-containing Iron(III) Oxide Adsorbents for Arsenic Removal, *Water Res.* **2004**, *37*, 4351.

[10] M. T. Emett, G. H. Khoe, Photochemical Oxidation of Arsenic by Oxygen and Iron in Acid Solution, *Water Res.* **2001**, *35*, 639.

[11] C. L. Chuang, M. Fan, R. C. Brown, S. Sung, B. Saha, C. P. Huang, Adsorption of Arsenic(V) by Activated Carbon Prepared from Oat Hulls, *Chemosphere* **2005**, *61*, 478.

[12] Y. Zhang, M. Yang, X. Huang, Arsenic(V) Removal with a Ce(IV)-Doped Iron Oxide Adsorbent, *Chemosphere* **2003**, *51*, 945.

[13] S. M. Fendorf, J. Eick, P. R. Grossl, D. L. Sparks, Arsenate and Chromate Retention Mechanisms on Geothite. 1 Surface Structure, *Environ. Sci. Technol.* **1997**, *31*, 315.

[14] Y. H. Xu, T. Nakajima, A. Ohki, Adsorption and Removal of Arsenic(V) from Drinking Water by Aluminium-loaded Shirasu-zeolite, *J. Hazard. Mater.* **2002**, *B92*, 275.

[15] X. Chen, G. Chen, P. L. Yue, Investigation on the Electrolysis Voltage of Electrocoagulation, *Chem. Eng. Sci.* **2002**, *57*, 2449.

[16] G. Chen, Electrochemical Technologies in Wastewater Treatment, *Sep. Purif. Technol.* **2004**, *38*, 11.

[17] N. Adhoum, L. Monser, Decolourization and Removal of Phenolic Compounds from Olive Mill Wastewater by Electrocoagulation, *Chem. Eng. Process.* **2004**, *43*, 1281.

[18] K. Rajeshwar, J. K. Ibanez, *Environmental Electrochemistry: Fundamentals and Applications in Pollution Abatement*, Academic Press, San Diego **1997**.

[19] E. A. Vik, D. A. Carlson, A. S. Eikum, E. T. Gjessing, Electroocoagulation of Potable Water, *Water Res.* **1984**, *18*, 1355.

[20] A. M. García-Lara, C. Montero-Ocampo, Improvement of Arsenic Electro-removal from Underground Water by Lowering the Interference of Other Ions, *Water Air Soil Pollut.* **2010**, *205*, 244.

[21] K. Thella, B. Verma, V. C. Srivastava, K. K. Srivastava, Electrocoagulation Study for the Removal of Arsenic and Chromium from Aqueous Solution, *J. Environ. Sci. Health Part A* **2008**, *43*, 554.

[22] N. Balasubramanian, T. Kojima, C. Srinivasakannan, Arsenic Removal through Electrocoagulation: Kinetic and Statistical Modeling, *Chem. Eng. J.* **2009**, *155*, 76.

[23] H. K. Hansen, P. Nunez, C. Jil, Removal of Arsenic from Wastewaters by Airlift Electrocoagulation. Part 1: Batch Reactor Experiments, *Sep. Purif. Technol.* **2008**, *43*, 224.

[24] M. Ikematsu, K. Kaneda, M. Iseki, M. Yasuda, Electrochemical Treatment of Human Urine for Its Storage and Reuse as Flush Water, *Sci. Total Environ.* **2007**, *382*, 159.

[25] S. Vasudevan, J. Lakshmi, G. Sozhan, Studies on the Removal of Iron from Drinking Water by Electrocoagulation – A Clean Process, *Clean* **2009**, *37*, 45.

[26] B. Manna, U. C. Ghosh, Adsorption of Arsenic from Aqueous Solution on Synthetic Hydrous Stannic Oxide, *J. Hazard. Mater.* **2007**, *144*, 522.

[27] E. Malkoc, Y. Nuhoglu, Potential of Tea Factory Waste for Cr(VI) Removal from Aqueous Solutions: Thermodynamic and Kinetic Studies, *Sep. Purif. Technol.* **2007**, *54*, 291.

[28] K. P. Raven, A. Jain, R. H. Loeppert, Arsenite and Arsenate Adsorption on Ferrihydride: Kinetics, Equilibrium and Adsorption Envelopes, *Environ. Sci. Technol.* **1998**, *32*, 344.

[29] D. Erhan, M. Kobya, S. Elif, T. Ozkan, Adsorption Kinetics for the Removal of Chromium III from Aqueous Solutions on the Activated Carbonaceous Prepared from Agricultural Wastes, *Water SA* **2004**, *30*, 533.

[30] I. A. Oke, N. O. Olarinoye, S. R. A. Adewusi, Adsorption Kinetics for Arsenic Removal from Aqueous Solutions by Untreated Powdered Eggshell, *Adsorption* **2008**, *14*, 73.

[31] W. J. Weber, J. C. Morris, Kinetics of Adsorption on Carbon from Solutions, *J. Sanit. Div. Am. Soc. Civ. Eng.* **1963**, *89*, 31.

[32] S. J. Allen, G. Mckay, K. H. Y. Khader, Intraparticle Diffusion of Basic Dye During Adsorption onto Sphagnum Peat, *Environ. Pollut.* **1989**, *56*, 39.

[33] M. S. Gasser, G. H. A. Morad, H. F. Aly, Batch Kinetics and Thermodynamics of Cr Ions Removal from Waste Solutions Using Synthetic Adsorbents, *J. Hazard. Mater.* **2007**, *142*, 118.

[34] M. Jaroniec, Current State in Adsorption from Multicomponent Solutions of Nonelectrolytes on Solids, *Adv. Colloid Interface Sci.* **1983**, *18*, 149.

[35] B. R. Manna, M. Dasgupta, U. C. Ghosh, Studies on Crystalline Hydrous Titanium Oxide (CHTO) as Scavenger of Arsenic(III) from Natural Water, *J. Water SRT-Aqua* **2004**, *53*, 483.

[36] B. R. Manna, S. Debnath, J. Hossain, U. C. Ghosh, Trace Arsenic Contaminated Groundwater Upgradation Using Hydrated Zirconium Oxide (HZO), *J. Ind. Pollut. Control* **2004**, *20*, 247.

[37] I. A. W. Tan, B. H. Hameed, A. L. Ahmed, Equilibrium and Kinetics Studies on the Basic Dye Adsorption by Palm Fibre Activated Carbon, *Chem. Eng. J.* **2007**, *127*, 111.

[38] H. Demiral, I. Demiral, F. Tumsek, B. Karacbacakoglu, Adsorption of Chromium(Vl) from Aqueous Solution by Activated Solution by Activated Carbon Derived from Olive Bagasse and Applicability of Different Adsorption Models, *Chem. Eng. J.* **2008**, *144*, 188.

[39] E. Oguz, Adsorption Characteristics and the Kinetics of the Cr(VI) on the Thuja Oriantalis, *Colloid Surf.* **2005**, *252*, 121.

[40] N. K. Lazaridis, D. N. Bakayannakis, E. A. Deliayanni, Chromium(VI) Sorptive Removal from Aqueous Solutions by Nanocrystalline Akaganeite, *Chemosphere* **2005**, *58*, 65.

[41] X. Y. Yang, B. Al-Duri, Application of Branched Pore Diffusion Model in the Adsorption of Reactive Dyes on Activated Carbon, *Chem. Eng. J.* **2001**, *83*, 15.

[42] A. K. Golder, A. N. Samantha, S. Ray, Removal of Phosphate from Aqueous Solution Using Calcined Metal Hydroxides Sludge Waste Generated from Electrocoagulation, *Sep. Purif. Technol.* **2006**, *52*, 102.

[43] A. G. J. Gomes, P. Daida, M. Kesmez, M. Weir, H. Moreno, R. J. Parga, G. Irwin, H. McWhinney, T. Grady, E. Peterson, L. D. Cocke, Arsenic Removal by Electrocoagulation Using Combined Al–Fe Electrode System and Characterization of Products, *J. Hazard. Mater.* **2007**, *B139*, 220.

[44] S. Bang, D. M. Johnson, P. G. Korfiatis, X. Meng, Chemical Reactions Between Arsenic and Zero-valent Iron in Water, *Water Res.* **2005**, *39*, 763.

